Geophysical Research Letters

Key Points:
- Observed acetaldehyde (CH_3CHO) in the remote troposphere is compatible with observed peroxyacetic acid (PAA) within uncertainties
- We speculate that there is a missing CH_3CHO source in the remote atmosphere and observed organic aerosols cannot explain the observed CH_3CHO
- The ocean is a net source of CH_3CHO; the ocean biogeochemistry control on the atmospheric chemistry warrants further investigation

Supporting Information:
- Supporting Information S1

Correspondence to:
S. Wang,
siyuan@ucar.edu

Atmospheric Acetaldehyde: Importance of Air-Sea Exchange and a Missing Source in the Remote Troposphere

Siyuan Wang[1,2], Rebecca S. Hornbrook[2], Alan Hills[2], Louisa K. Emmons[2], Simone Tilmes[2,3], Jean-François Lamarque[2,3], Jose L. Jimenez[4,5], Pedro Campuzano-Jost[4,5], Benjamin A. Nault[4,5], John D. Crounse[6], Paul O. Wennberg[6], Michelle Kim[6], Hannah Allen[6], Thomas B. Ryerson[7], Chelsea R. Thompson[5,7], Jeff Peischl[5,7], Fred Moore[7], David Nance[7], Brad Hall[7], James Elkins[7], David Tanner[8], L. Gregory Huey[8], Samuel R. Hall[2], Kirk Ullmann[2], John J. Orlando[2], Geoff S. Tyndall[2], Frank M. Flocke[2], Eric Ray[7], Thomas F. Hanisco[9], Glenn M. Wolfe[9,10], Jason St. Clair[9,10], Róisín Commane[11,12], Bruce Daube[11], Barbara Barletta[13], Donald R. Blake[13], Bernadett Weinzierl[14], Maximilian Dollner[14], Andrew Conley[2], Francis Vitt[2], Steven C. Wofsy[11], Daniel D. Riemer[15], and Eric C. Apel[2]

[1]Advanced Study Program, National Center for Atmospheric Research, Boulder, CO, USA, [2]Atmospheric Chemistry Observations and Modeling, National Center for Atmospheric Research, Boulder, CO, USA, [3]Climate and Global Dynamics, National Center for Atmospheric Research, Boulder, CO, USA, [4]Department of Chemistry and Biochemistry, University of Colorado Boulder, Boulder, CO, USA, [5]Cooperative Institute for Research in the Environmental Sciences, University of Colorado Boulder, Boulder, CO, USA, [6]Division of Engineering and Applied Science and Division of Geological and Planetary Sciences, California Institute of Technology, Pasadena, CA, USA, [7]Earth System Research Laboratory, National Oceanic and Atmospheric Administration, Boulder, CO, USA, [8]School of Earth and Atmospheric Sciences, Georgia Institute of Technology, Atlanta, GA, USA, [9]Goddard Space Flight Center, National Aeronautics and Space Administration, Greenbelt, MD, USA, [10]Joint Center for Earth Systems Technology, University of Maryland, Baltimore County, Baltimore, MD, USA, [11]Harvard School of Engineering and Applied Sciences, Department of Earth and Planetary Sciences, Harvard University, Cambridge, MA, USA, [12]Department of Earth and Environmental Sciences, Lamont-Doherty Earth Observatory, Columbia University, New York, NY, USA, [13]Department of Chemistry, University of California, Irvine, CA, USA, [14]Faculty of Physics, Aerosol Physics and Environmental Physics, University of Vienna, Wien, Austria, [15]Apel-Riemer, Environmental Inc., Miami, FL, USA

Abstract We report airborne measurements of acetaldehyde (CH_3CHO) during the first and second deployments of the National Aeronautics and Space Administration Atmospheric Tomography Mission (ATom). The budget of CH_3CHO is examined using the Community Atmospheric Model with chemistry (CAM-chem), with a newly developed online air-sea exchange module. The upper limit of the global ocean net emission of CH_3CHO is estimated to be 34 Tg/a (42 Tg/a if considering bubble-mediated transfer), and the ocean impacts on tropospheric CH_3CHO are mostly confined to the marine boundary layer. Our analysis suggests that there is an unaccounted CH_3CHO source in the remote troposphere and that organic aerosols can only provide a fraction of this missing source. We propose that peroxyacetic acid is an ideal indicator of the rapid CH_3CHO production in the remote troposphere. The higher-than-expected CH_3CHO measurements represent a missing sink of hydroxyl radicals (and halogen radical) in current chemistry-climate models.

Plain Language Summary The Earth's atmosphere and its ability to self-regulate and cleanse itself is dependent on a complex interplay of trace chemical species, some of which are emitted from the biosphere, while others are from human activities or fires. One of these key species, acetaldehyde, was measured as part of the recent Atmospheric Tomography Mission, an aircraft (National Aeronautics and Space Administration DC-8) experiment transecting the lengths of the Pacific and Atlantic Oceans during two seasons, measuring greenhouse gases and chemically reactive gases and particles. These measurements allow us to test our ability to model the chemical state of the atmosphere. The results indicate that the ocean is a large source of acetaldehyde and the analysis here suggests additional mechanisms that narrow the gap between observations and simulations but also reveal that an additional unexplained source or sources remain(s) in the remote free troposphere. It is critical to understand this missing carbon source because it has

significant implications for understanding the cycle of oxidants which, in turn, provide for the means of removing (cleaning) trace gases including methane, an important greenhouse gas, from the atmosphere.

1. Introduction

Acetaldehyde is one of the most abundant oxygenated volatile organic compounds (OVOCs) in the atmosphere. It is a major precursor of peroxyacetyl nitrate (PAN; Fischer et al., 2014), which affects the long-range transport of NO_x ($NO + NO_2$; Singh et al., 1990). It also affects hydrogen oxide radicals (Moxim et al., 1996; Seinfeld & Pandis, 2012) and reactive halogen chemistry (Hornbrook et al., 2016; Koenig et al., 2017). High levels of CH_3CHO have been reported in the remote marine boundary layer (MBL; Read et al., 2012; Singh et al., 2003) and the free troposphere (FT; Singh et al., 2001, 2003). However, it has been suspected that the early in situ CH_3CHO measurements may have been subject to sampling artifacts, with the largest impacts in the remote FT (Apel et al., 2008; Bates et al., 2000; Goldan et al., 2004; Millet et al., 2010; Northway et al., 2004). Evidence to support that suspicion in the remote FT is provided by the concomitant PAN measurements, with the observed PAN and CH_3CHO mutually incompatible based on their known chemistry (Millet et al., 2010; Staudt et al., 2003). Progress has been made in recent years to quantify trace levels of CH_3CHO in pristine environments using the NCAR Trace Organic Gas Analyzer (TOGA; see more details in the supporting information, SI; Apel et al., 2003, 2015; Hornbrook et al., 2016).

The ocean is the biggest organic carbon reservoir on the surface of the Earth (Ogawa & Tanoue, 2003). Colored dissolved organic matter (CDOM) in a variety of natural waters absorbs ultraviolet radiation (i.e., 280–320 nm), producing a number of low-molecular-weight compounds, including CH_3CHO (Kieber et al., 1990, 2003; Mopper et al., 1991). CH_3CHO produced in the surface seawater is rapidly consumed via microbial processes (Dixon et al., 2013; Mopper & Stahovec, 1986). Using a global chemical transport model (GEOS-Chem), Millet et al. (2010) conducted pioneering work on quantifying oceanic emissions of CH_3CHO. However, at that time the modeled surface seawater concentrations and oceanic fluxes of CH_3CHO were largely untested with observations.

In this work, we use a global chemistry-climate model (CESM2.1/Community Atmospheric Model with chemistry [CAM-chem]) to test our current understanding of CH_3CHO budget in the remote atmosphere. This includes the air-sea exchange of CH_3CHO which is examined in the context of all previous oceanic observations (surface seawater concentrations and fluxes) available in the literature. In situ measurements of CH_3CHO during the first and second deployments of the recent Atmospheric Tomography Mission (ATom-1 and ATom-2) were used for model evaluation.

2. Methods

The ATom-1 and ATom-2 missions took place from 29 July to 23 August 2016 and 26 January to 21 February 2017, respectively. In this work we focus on the flights over the Pacific Ocean. During ATom-1 and ATom-2, air masses probed over the Atlantic were frequently affected by biomass burning, as indicated by elevated HCN, CH_3CN, and CO. Chemical evolution of organic compounds in biomass burning plumes remains poorly understood. The scope of this work is to examine the budget of CH_3CHO in the pristine air over the Pacific; therefore, flights over the Atlantic were not included in this work. OVOCs were measured using the TOGA instrument (see more details in SI and Figure S1 and S2), and other observations involved in this work are listed in the SI. The flight tracks are shown in Figures S3–S5.

2.1. CESM2.1/CAM-Chem

CAM-chem is a component of the Community Earth System Model (CESM; Lamarque et al., 2012; Tilmes et al., 2015). In this work, CAM-chem is run in an off-line configuration (with specified dynamics), using National Aeronautics and Space Administration (NASA) MERRA2 (reanalysis) meteorology fields with a horizontal resolution of 0.94° latitude × 1.25° longitude and 32 levels (surface to 3 hPa). The chemistry scheme includes a detailed representation of tropospheric and stratospheric chemistry (Tilmes et al., 2015). Anthropogenic emissions are from the Coupled Model Intercomparison Project Phase 6 (CMIP6; Hoesly et al., 2018), biomass burning emissions are from the Fire INventory version 1.5 for NCAR (FINN;

Wiedinmyer et al., 2011), and terrestrial emissions are calculated using the Model of Emissions of Gases and Aerosols from Nature (MEGAN; Guenther et al., 2012).

2.2. Air-Sea Exchange for Trace Gases

An Online Air-Sea Interface for Soluble Species (OASISS) was developed for CAM-chem to calculate the bidirectional oceanic fluxes of trace gases (Johnson, 2010; Liss & Slater, 1974). In brief, the air-sea exchange is described by the air-side and water-side transfer velocities (k_{air} and k_{water}). The k_{air} is based on the NOAA COARE algorithm (Jeffery et al., 2010), with the addition of the still air diffusive flux adjustment (Mackay & Yeun, 1983). The k_{water} is based on Nightingale et al. (2000). The air-sea exchange of a given gas is determined by its concentrations in the surface seawater and the atmosphere, as well as its (effective) Henry's law constant. For CH_3CHO, its effective Henry's law constant (12 M/atm at 298 K) is used in this work, considering its hydration in the aqueous phase (Betterton & Hoffmann, 1988). In addition, the bubble-mediated transfer due to white caps (Asher & Wanninkhof, 1998) is included in the framework as an option, in which the fractional coverage of actively breaking whitecaps is parameterized based on a previous study (Soloviev & Schluessel, 2002). In this work, the bubble-mediated transfer is turned off unless otherwise noted. The surface seawater salinity is obtained from the NASA SAC-D/Aquarius level-3 monthly climatology (Lee et al., 2012). The parameterization of the CH_3CHO seawater concentration is described in the following section.

2.3. Simplified Ocean Biogeochemistry Scheme for CH_3CHO

The seawater concentration of CH_3CHO is estimated using a satellite-based approach similar to (Millet et al., 2010). In brief, due to the short biological turnover time of CH_3CHO (<1 day) in the surface seawater (Dixon et al., 2013; Mopper et al., 1991; Zhou & Mopper, 1997), surface seawater CH_3CHO is assumed to be in steady state, and hence, its steady state concentration can be estimated based on production rate (Kieber et al., 1990) and the turnover time. Kieber et al. (1990) measured the CH_3CHO production from the UV photolysis of CDOM obtained from natural water samples, and parameterized the production rate as a function of CDOM absorption coefficient at 300 nm. In this work, the NASA SeaWiFS level-3 product, the monthly climatology of absorption coefficient due to colored dissolved and detrital organic matter at 443 nm (Maritorena et al., 2002), is used to estimate the CDOM absorption (a_{CDOM}) and attenuation (k_d) at 300 nm using a linear regression method (Swan et al., 2009).

The local CH_3CHO production rate within the ocean mixed layer can then be calculated using $a_{CDOM,300\ nm}$, $k_{d,300\ nm}$, the total UV radiation (280–320 nm) absorbed by the ocean (CAM-chem), and the acetaldehyde production rate reported by Kieber et al. (1990). The ocean mixed layer depth is from the NCAR Large Ensemble Community Project (Kay et al., 2014). A constant turnover time (0.3 day) is used throughout the ocean mixed layer (Dixon et al., 2013; also see details in SI); therefore, the resulting steady state CH_3CHO concentration is an average throughout the ocean mixed layer.

2.4. Observation-Based Box Model

An observationally constrained photochemical box model (Wang et al., 2015) is also used to examine sources and sinks of CH_3CHO. A near-explicit gas-phase chemical mechanism, Master Chemical Mechanism v3.3.1 (Jenkin et al., 2003), is used, with the addition of the reaction ($CH_3O_2\cdot + OH$) included based on recent findings (Assaf et al., 2017; Bossolasco et al., 2014). The box model is constrained to all measurements available, for example, j values (Shetter & Müller, 1999), water vapor (Diskin et al., 2002), NO (Ryerson et al., 2000), CO (McManus et al., 2005), H_2 and PAN (Elkins et al., 1996), methane (Crosson, 2008), and formaldehyde (Cazorla et al., 2015). See SI for more details.

3. Surface Seawater Concentration of CH_3CHO

The few published seawater measurements of CH_3CHO range from below detection limits (mostly <2 nM) to 30 nM (Beale et al., 2013, 2015; Dixon et al., 2013; Kameyama et al., 2010; Mopper et al., 1991; Mopper & Stahovec, 1986; Schlundt et al., 2017; Yang et al., 2014; Zhou & Mopper, 1997). Figure S6 shows the modeled surface seawater concentrations of CH_3CHO, as well as all aforementioned surface seawater measurements. Note that Zhou and Mopper (1997) measured CH_3CHO in both bulk seawater (1.4 ± 0.1 nM) and the surface microlayer (15.7 ± 2.2 nM), while all other studies reported bulk surface seawater. For consistency, bulk seawater measurements from Zhou and Mopper (1997) are plotted here. As shown in Figure S6, the modeled

seawater concentrations of CH_3CHO cover a similar range as most of the observations in the open oceans, especially with the AMT cruise observations in the Atlantic (Beale et al., 2013; Yang et al., 2014), spanning from 50°N to 45°N. The air-sea exchange of CH_3CHO is fully coupled with the chemical and physical processes in the atmosphere, and the oceanic fluxes will respond to the production and removal mechanisms in the atmosphere (section 6); therefore, the modeled oceanic fluxes are discussed in section 7 in the context of CH_3CHO chemistry in the atmosphere.

4. Peroxyacetic Acid as an Indicator of CH_3CHO in the Remote Atmosphere

Previous studies have used PAN as an indicator of CH_3CHO (Millet et al., 2010; Staudt et al., 2003). However, NO_2 is another direct precursor of PAN, and the low-NO_x air masses probed during the ATom flights do not favor the formation of PAN. Moreover, PAN is much longer-lived than CH_3CHO and hence is less indicative of the rapid local turnover of CH_3CHO. In light of this, we propose that peroxyacetic acid (PAA) is an ideal indicator for CH_3CHO in the remote atmosphere, because (i) CH_3CHO is the dominant precursor of PAA; (ii) the chemical lifetime of PAA is a few days, and hence is less affected by long-range transport and convection; and (iii) the formation mechanism of PAA is more relevant in pristine air with very low NO_x content. Using an observationally constrained box model, we found that the observed CH_3CHO can possibly explain all the PAA measurements (CIT ToF-CIMS; Crounse et al., 2006; see the SI for details) which is otherwise drastically underestimated (Figure S7). PAA measurements were not available in most previous studies. The simultaneous measurements of PAA provide strong support for the veracity of the observed CH_3CHO mixing ratios in the remote troposphere, which is an observational advance permitting new chemical insights.

5. Measured and Modeled Acetaldehyde Vertical Profiles

Figure 1 shows the vertical distribution of TOGA-measured CH_3CHO over the remote Pacific during ATom-1 and ATom-2, as well as model simulations in which the model outputs were sampled along the flight tracks. Anthropogenic (CO and NO as indicators), biomass burning (HCN and CH_3CN as indicators), stratospheric (indicated by O_3), and cloud (flagged by the onboard Cloud, Aerosol, and Precipitation Spectrometer) influences were all filtered out, so that the observations reflect cloud-free clean air conditions. The latitudinal distributions of CO, NO, O_3, and HCN, from both raw and filtered measurements, are shown in Figures S4 and S5.

The observed CH_3CHO shows both spatial and seasonal variations: During ATom-1 (July–August 2016), observed CH_3CHO reached 200–400 pptv in the MBL in the NH and tropical Pacific, while slightly lower levels, 100–350 pptv, were observed in the MBL in the SH Pacific. Above the MBL, observed CH_3CHO decreased gradually with increasing height, and above ~10 km the majority of observations dropped close to or below the TOGA detection limit (5 pptv). Table S2 summarizes all CAM-chem scenarios in this work. Without oceanic fluxes, the CAM-chem simulation underestimated CH_3CHO in the MBL in all regions, and underestimated CH_3CHO by 1 order of magnitude in the FT in the NH and tropical Pacific (red lines in Figure 1). With the oceanic fluxes (blue lines in Figure 1), CAM-chem CH_3CHO in the MBL is greatly improved, but the impact of oceanic emissions in the FT is limited. The findings from ATom-2 (January–February 2017) generally mirror those from ATom-1.

Air mass history analysis indicated that the FT air masses probed during ATom have not been influenced by the marine/planetary boundary layer for at least two days prior being sampled on the aircraft (Figure S8). Uncertainties in CAM-chem modeled OH radicals are unlikely to explain all the underestimation in CH_3CHO, since CAM-chem predicted OH radicals in the remote troposphere agree with ATHOS measurements (Faloona et al., 2004) within 23% (Pearson coefficients: 0.79 and 0.76 for ATom-1 and ATom-2, respectively). CAM-chem predicted ethane (a major CH_3CHO precursor) agrees with the UCI WAS measurements (Blake et al., 2003) within 33–68% in the remote troposphere during ATom (except for NH winter when CAM-chem underestimates by up to a factor of ~2), implying that the large underestimation of CAM-chem CH_3CHO cannot be all explained by ethane. Analysis of tagged CH_3CHO tracers (anthropogenic, terrestrial, oceanic, biomass burning, and secondary productions) in CAM-chem indicates that convective transport plays a minor role in the CH_3CHO budget in the remote troposphere (up to 30% in the upper FT over the
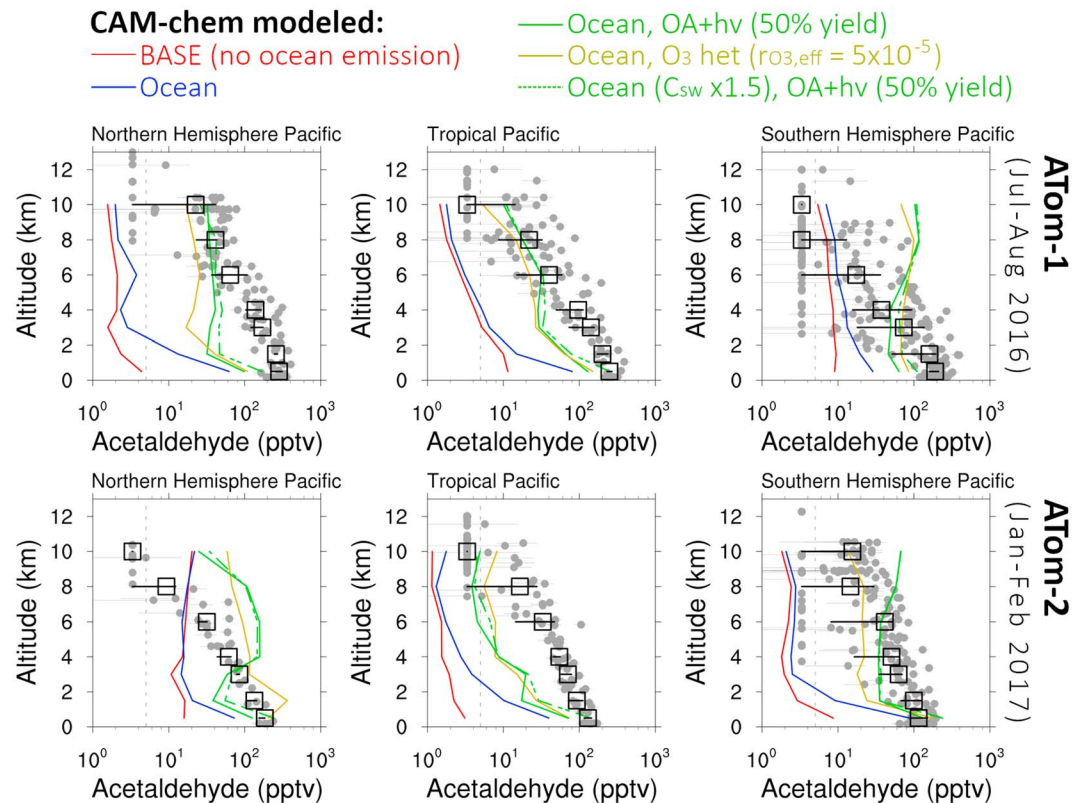
Figure 1. TOGA measured CH_3CHO in the Northern Hemisphere (>10°N), tropical (10°N–10°S), and Southern Hemisphere (<10°S) over the remote Pacific Ocean during ATom-1 (top) and ATom-2 (bottom). Grey dots are 2-min TOGA measurements and black boxes are the median profiles (with 25% and 75% percentiles shown as thick black bars). Light grey error bars represent TOGA measurement uncertainties for CH_3CHO (20% + 10 pptv). Dashed vertical lines indicate the TOGA detection limit (DL) for CH_3CHO (5 pptv), and measurements below DL are shown as one half of DL. Red lines are CAM-chem base case simulation, while blue lines show the CAM-chem simulation with oceanic emissions. Green represents radiation-driven CH_3CHO production from OA (with a 50% CH_3CHO yield), while yellow represents O_3-induced CH_3CHO production from OA, and dashed green lines represent simulations with 50% higher seawater concentration and radiation-driven CH_3CHO production from OA (otherwise same as green).

Western Pacific which was not the target region of ATom). Moreover, Figure S9 shows that the TOGA-measured dimethyl sulfide (another short-lived ocean emitted tracer) vertical gradient profile in the MBL is reasonably captured by CAM-chem providing evidence that CAM-chem likely does not significantly underestimate the convective transport into the FT (section S5). The tagged tracer analysis also indicates that terrestrial CH_3CHO emissions contribute negligible amounts of CH_3CHO in the remote troposphere (including CH_3CHO produced from isoprene and terpenes). However, we cannot rule out the possibility that CH_3CHO may be produced during the aging processes of organic compounds emitted from the terrestrial biosphere. Moreover, a photochemical steady state model constrained to all VOC measurements available (including all C1–C4 hydrocarbons and OVOCs, isoprene, benzene, and toluene; see Table S1) can explain less than 10% of the TOGA measured CH_3CHO, consistent with our findings using CAM-chem. Given the short chemical lifetime of CH_3CHO (a few hours; mainly OH oxidation, and to a lesser extent, photolysis), our analysis strongly suggests a missing source of CH_3CHO in the pristine tropospheric air. The oceanic influence is mostly confined within the lowest 3–4 km (above the ocean), and the modeled CH_3CHO vertical profiles with oceanic influence show a steeper vertical gradient in the lowest 3–4 km, compared to observations. This implies the missing source plays a role in the MBL as well. Interestingly, the missing source appears to be at least partially radiation-driven, as the measured CH_3CHO can be reasonably captured by the model in the winter hemisphere (ATom-1 SH and ATom-2 NH) but not in the summer hemisphere (ATom-1 NH and ATom-2 SH). Note that in the wintertime NH upper FT, CH_3CHO was overestimated in the CAM-chem base case simulation without oceanic emissions.

6. On the Currently Missing CH₃CHO Production Mechanisms

In this section we explore the possible mechanisms to explain the underestimated CH_3CHO based on observations. Due to its short chemical lifetime, CH_3CHO in the remote troposphere can be assumed in steady state. The observationally derived instantaneous removal rate as well as the inferred production rate of CH_3CHO are then given by

$$\frac{d[CH_3CHO]}{dt}\bigg|_{source} \approx \frac{d[CH_3CHO]}{dt}\bigg|_{sink} = [CH_3CHO]\cdot\big(j_{CH_3CHO} + k_{CH_3CHO+OH}[OH]\big) \tag{1}$$

where $[CH_3CHO]$ and $[OH]$ are the observed concentrations of CH_3CHO and OH, j_{CH3CHO} is the CH_3CHO photolysis frequency calculated from the actinic flux measurements, and $k_{CH3CHO\ +\ OH}$ is the OH reaction rate coefficient (Burkholder et al., 2015). Two hypothesized CH_3CHO production mechanisms are examined:

1. Light-driven CH_3CHO production from organic aerosols (OA), motivated by laboratory studies (Chiu et al., 2017; Kieber et al., 1990), in which UV photolysis of organic substances produces carbonyl compounds:
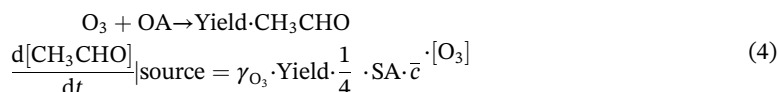
$$OA + h\nu \rightarrow Yield\cdot CH_3CHO$$
$$\frac{d[CH_3CHO]}{dt}\bigg|source = j_{OA}\cdot Yield\ \cdot[OA] \tag{2}$$
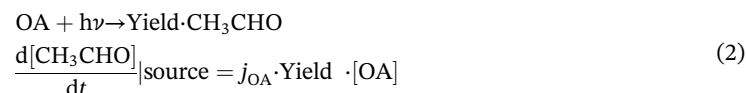
where $[OA]$ is the organic aerosol mass concentration ($\mu g/m^3$), j_{OA} is the photolysis frequency of organic aerosol (s), and *Yield* is the stoichiometric yield of CH_3CHO. If we plug equation (2) into equation (1) and use micrograms per cubic meter per second as the units for $\frac{d[CH_3CHO]}{dt}$, then the observationally derived CH_3CHO loss rate corresponds to an OA lifetime of

$$\text{Inferred OA lifetime (day)} = \frac{[OA]}{\frac{d[CH_3CHO]}{dt}} \approx \frac{[OA]}{[CH_3CHO]\cdot\big(j_{CH_3CHO} + k_{CH_3CHO+OH}[OH]\big)} \cdot \frac{3}{86,400}. \tag{3}$$

where the factor 3 (on the right-hand side of equation (3)) roughly converts the instantaneous lifetime to 24-hr average lifetime, and 86,400 converts the unit of lifetime from seconds to days. It is assumed here that OA is converted into CH_3CHO at 100% carbon yield (upper limit to possible CH_3CHO production).

2. Ozonolysis of organic aerosols, also motivated by laboratory studies (Molina et al., 2004; Rudich, 2003; Thornberry & Abbatt, 2004), in which reactive uptake of O_3 on organic substances produces low molecular weight VOCs:

$$O_3 + OA \rightarrow Yield\cdot CH_3CHO$$
$$\frac{d[CH_3CHO]}{dt}\bigg|source = \gamma_{O_3}\cdot Yield\cdot\frac{1}{4}\ \cdot SA\cdot\bar{c}\ \cdot[O_3] \tag{4}$$

where γ_{O3} is the reactive uptake coefficient of O_3, SA is the measured total aerosol surface area (cm^2/cm^3), $\bar{c}$ is the molecular speed (cm/s), $[O_3]$ is the O_3 concentration ($molec/cm^3$), and the term $\frac{1}{4}\cdot SA\cdot\bar{c}\cdot[O_3]$ is the O_3 collision rate ($molec\cdot cm^{-3}\cdot s^{-1}$). Plugging equation (1) into equation (4), the observationally derived CH_3CHO loss rate corresponds to an effective O_3 uptake coefficient of

$$\text{Inferred } O_3 \text{ uptake} = \gamma_{O_3}\cdot Yield = \frac{[CH_3CHO]\cdot\big(j_{CH_3CHO} + k_{CH_3CHO+OH}[OH]\big)}{\frac{1}{4}\cdot SA\cdot\bar{c}\cdot[O_3]} \tag{5}$$

The formulation of equation (5) does not need to specify the yield, as the right-hand side term $\left(\frac{[CH_3CHO]\cdot\big(j_{CH_3CHO} + k_{CH_3CHO+OH}[OH]\big)}{\frac{1}{4}\cdot SA\cdot\bar{c}\cdot[O_3]}\right)$ is factually the product between the reactive uptake coefficient and the yield (i.e., $\gamma_{O3}\cdot Yield$). Equations (3) and (5) are both purely observationally constrained and therefore are not affected by model uncertainties. HR-AMS-measured PM_1 OA mass concentration (DeCarlo et al., 2006; Nault et al., 2018; Schroder et al., 2018) is used in equation (3), and total aerosol surface area
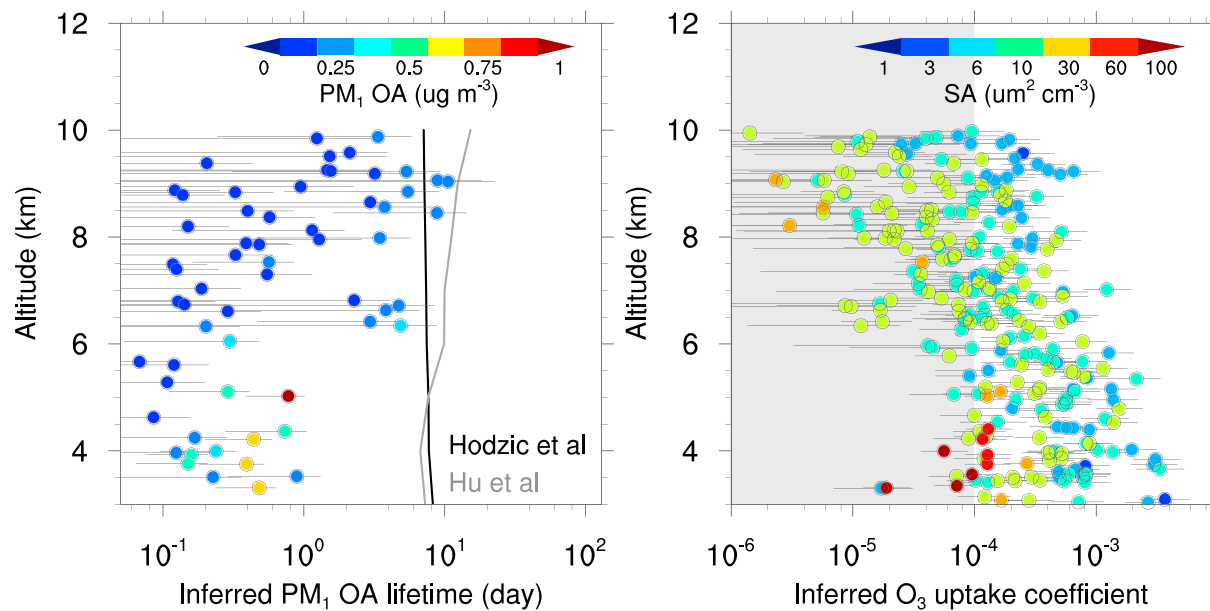
Figure 2. (left) OA lifetime and (right) O_3 uptake coefficient inferred from CH_3CHO measurements in the FT, color coded by HR-AMS measured PM_1 OA mass concentration (left) and observed total aerosol surface area density (right). Temperature-dependent kinetic uncertainty of the CH_3CHO + OH reaction as well as all measurement uncertainties are propagated into the error bars. Solid lines in the left panel indicate fine particle lifetimes calculated based on Hodzic et al. (2016) and Hu et al. (2016). Grey shading in the right panel indicates the plausible range of O_3 uptake coefficient in the literature (Molina et al., 2004; Rudich, 2003; Thornberry & Abbatt, 2004).

(nucleation, Aitken, accumulation modes) calculated from AMP measurements (Brock et al., 2000; Kupc et al., 2018; Williamson et al., 2018) is used in equation (5). Figure 2 shows the combined results from both ATom-1 and ATom-2, excluding measurements below 3 km (where oceanic emissions play an important role). The TOGA-observed CH_3CHO implies a source strength of 1.7×10^{-3} ppt/s above 8 km and 3.2×10^{-3} ppt/s between 3 and 8 km (or 1.2×10^{-6} and 3.1×10^{-6} $\mu g \cdot m^{-3} \cdot s^{-1}$, respectively; all instantaneous rates). As shown in this figure, if hypothesis (i) is solely responsible for the missing CH_3CHO source in the remote FT, the observationally derived CH_3CHO loss rate corresponds to an OA lifetime ranging from ~1 day in the lower-middle FT (<8 km) to ~10 days in the upper FT (>8 km). Similarly, if hypothesis (ii) is solely responsible for the missing CH_3CHO in the remote FT, the observationally derived CH_3CHO loss rate corresponds to an O_3 uptake coefficient on the order of ~10^{-3} in the lower-middle FT (<8 km) to ~10^{-5} in the upper FT (>8 km).

Previous studies have indicated that the OA lifetime in the remote FT is likely of the order of ~10 days (Hodzic et al., 2016; Hu et al., 2016), much longer than what is required to explain the observed CH_3CHO. Similarly, laboratory studies found that the O_3 uptake coefficient on various organic substances is typically 10^{-4} or less (Molina et al., 2004; Rudich, 2003; Thornberry & Abbatt, 2004). However, to explain the observed CH_3CHO below <8 km, an O_3 uptake coefficient much larger than 10^{-4} is required, which appears to be unrealistic. These results indicate that organic aerosols are insufficient to explain all the missing CH_3CHO especially in the FT.

These hypotheses were also tested in CAM-chem, and the modeled CH_3CHO vertical profiles with these hypotheses (both include oceanic emissions) are plotted in Figure 1 along with the previously discussed simulations:

1. Photolysis-driven CH_3CHO production from organic aerosols, and the photolytic loss of OA, is scaled to modeled j_{NO2}, leading to a mean daytime OA lifetime of ~9 days. The photolytic removal of organic aerosols in CAM-chem is the same as Hodzic et al. (2016). The yield of CH_3CHO from OA photolysis included in this study is assumed to be 50% (on a carbon basis), which leads to overall the best agreement in the upper FT, except for the cold seasons. Previous studies indicated that CAM-chem tends to transport

PAN and its precursors, including acetaldehyde, into higher altitude more rapidly in the source region especially in cold seasons (Arnold et al., 2015; Emmons et al., 2015). This may explain the higher CAM-chem CH_3CHO in the SH during ATom-1 and NH during ATom-2. The OA-photolysis-driven CH_3CHO production mechanism yields better spatial patterns of the oceanic fluxes (see section 7 for more details). Moreover, the OA-photolysis-driven CH_3CHO production (green line in Figure 1) also yields reasonable agreement in the upper FT compared to observations (mostly within a factor of 2, except for winter NH and summer SH when CH_3CHO is overestimated in the upper FT by a factor of 8–20), while in the lower-middle FT and MBL, the model still underestimates CH_3CHO. An additional sensitivity test with 50% higher seawater CH_3CHO concentration plus the additional CH_3CHO formation from OA photolysis (as described above) was also performed (dashed green lines in Figure 1), and this scenario leads to up to ~70% higher CH_3CHO and yields the best CH_3CHO agreement within the MBL. Note that in this scenario, the enhancements in seawater concentration (50%) and the resulting MBL CH_3CHO (up to 70%) are both smaller than the uncertainty of the air-sea exchange framework, which is on the order of 200%, possibly larger (Carpenter & Nightingale, 2015; Johnson, 2010).

2. CH_3CHO production from ozonolysis of OA, with an effective O_3 uptake coefficient of 5×10^{-5}, based on previous laboratory studies (Molina et al., 2004; Rudich, 2003; Thornberry & Abbatt, 2004). This scenario predicts that the high-latitude northern Atlantic and Pacific and Southern Oceans (both Pacific and Atlantic) are a net sink for CH_3CHO (Figure S11), which is inconsistent with available flux observations (Kieber et al., 1990; Yang et al., 2014).

In summary, we hypothesize that the gas-phase CH_3CHO precursors in the lower troposphere are currently not captured by measurements or models. It is plausible that other OVOCs might be produced along with CH_3CHO as well. For example, previous studies indicated that the origin of formaldehyde (Anderson et al., 2017; Baida et al., 2019) and glyoxal (Coburn et al., 2014; Volkamer et al., 2015) in the remote troposphere remain unexplained. There was a total OH reactivity (OHR) measurement onboard but the low OHR observed in the remote FT during ATom presents analytical challenges even for current state-of-the-art instruments; our hypothesis that gas-phase CH_3CHO precursors are required cannot be informed by comparisons of total measured versus calculated OHR because of the uncertainty in the measured OHR (~0.3 s) in the background troposphere. The CH_3CHO measurements in the MBL can be explained by a ~50% enhancement of surface seawater concentration, which may imply a surface microlayer enrichment (relative to bulk surface seawater) as suggested by Zhou and Mopper (1997), although the uncertainties in the air-sea exchange framework (Carpenter & Nightingale, 2015) may well give rise to an ~50% increase in the flux for a given seawater concentration.

7. Oceanic Flux of CH_3CHO

Although our analysis of missing CH_3CHO production (section 6) focused on the FT, it may occur in the MBL as well, which is consistent with the less-than-expected vertical gradient in the MBL CH_3CHO observations. The missing CH_3CHO source(s) in the atmosphere affects its air-sea exchange as well; for example, additional CH_3CHO production in the atmosphere shifts the air-sea equilibrium toward the ocean side. In this section we examine the modeled oceanic fluxes of CH_3CHO with previous flux measurements.

Measurements of oceanic flux of CH_3CHO are rare, especially in the Pacific. Most studies calculate the oceanic flux using measurements in both seawater and the atmosphere (Beale et al., 2013; Schlundt et al., 2017; Zhou & Mopper, 1997). Sinha and coworkers reported the net CH_3CHO flux in a mesocosm system near the Norwegian Sea (Sinha et al., 2007). Yang et al. (2014) reported the oceanic flux of CH_3CHO across the Atlantic using the eddy covariance method, which is to our knowledge the only study reporting the flux measurements of this type. Most studies report net upward CH_3CHO fluxes, up to 5×10^9 molec·cm^{-2}·s^{-1} over the open Atlantic ocean (Yang et al., 2014) and 12×10^9 molec·cm^{-2}·s^{-1} 100 km east of Bahamas (Zhou & Mopper, 1997), while Schlundt et al. reported a downward flux, up to -105×10^9 molec·cm^{-2}·s^{-1} (median: -7×10^9 molec·cm^{-2}·s^{-1}) in the South China Sea (Schlundt et al., 2017) due to high concentration in the air (median: 860 ppt). Figure 3 summarizes all previous oceanic CH_3CHO flux measurements, as well as the modeled fluxes using 50% higher seawater concentrations; also, included in the model is the radiation-driven CH_3CHO production from OA. As discussed in section 6, this scenario yields the overall best agreement in the MBL. As shown in Figure 3, the model predicts that the global ocean is generally a net source of
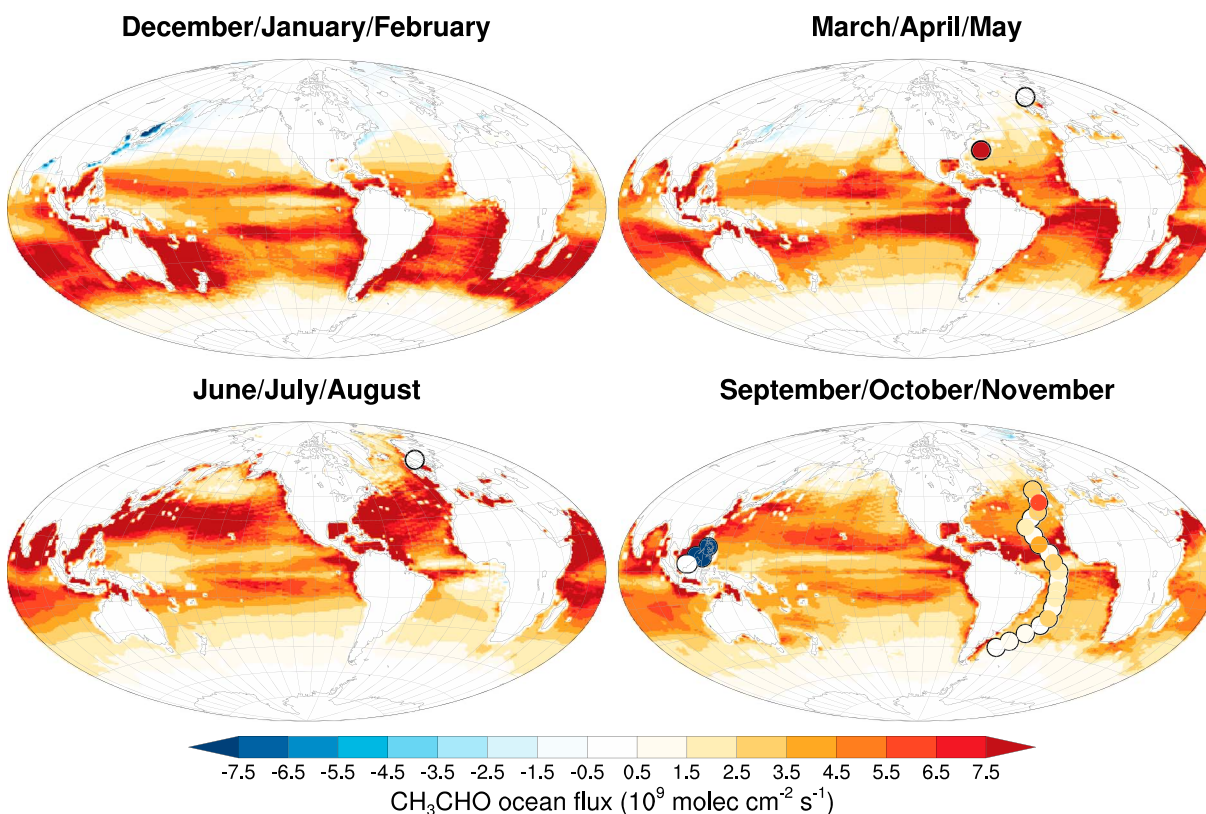
Figure 3. Modeled ocean-to-air flux of CH$_3$CHO. This model scenario is the same as the dashed green lines in Figure 1: oceanic emissions are calculated with 50% higher surface seawater CH$_3$CHO concentrations, and radiation-induced CH$_3$CHO production from OA is included as well. Flux measurements available in the literature are shown as circles.

CH$_3$CHO. The modeled oceanic flux of CH$_3$CHO is generally consistent with the flux observations, except for the fluxes reported in the South China Sea (Schlundt et al., 2017), because the high atmospheric CH$_3$CHO observed in that region was not captured by the model. The global annual net oceanic emission of CH$_3$CHO in this scenario is 34 Tg/a, which is increased to 42 Tg/a if the bubble-mediated transfer is considered. The bubble-mediated transfer has a bigger impact in the Southern Ocean, where stronger winds are frequently observed. The modeled global oceanic emission of CH$_3$CHO in this work is comparable to previous studies (Millet et al., 2010; Read et al., 2012). We consider the oceanic emissions of CH$_3$CHO estimated in this work to be the upper limit, as the unaccounted production mechanism(s) in the atmosphere will likely enhance the ocean uptake. Modeled oceanic fluxes of CH$_3$CHO for other modeling scenarios are provided in Figures S10 and S11.

8. Summary

In this study, an online air-sea exchange model framework is developed for CESM2.1/CAM-chem, and is combined with a simple ocean biogeochemistry scheme for CH$_3$CHO (Millet et al., 2010) to evaluate the CH$_3$CHO budget in the remote atmosphere. The modeled surface seawater concentrations and the oceanic fluxes of CH$_3$CHO are compared to all measurements available in the literature. Airborne measurements of CH$_3$CHO using TOGA during ATom-1 and ATom-2 are used for model evaluation. Balancing the evidence from the available oceanic flux measurements in the literature and vertical profile measurements, we estimated that the global ocean is a net source of CH$_3$CHO, with an annual net oceanic emission of 34–42 Tg/a (upper limit). Unfortunately, very few oceanic observations are available for model evaluation, and there is almost a complete lack of seawater concentrations and flux observations in the majority of Pacific. We suggest that future ship-based studies should target these regions for a better understanding of the air-sea exchange of CH$_3$CHO and other OVOCs.

We found that the observed CH_3CHO in the remote troposphere is underestimated by the default configuration of CAM-chem, implying a missing CH_3CHO source in the remote troposphere which is supported by the simultaneous measurements of PAA. We further show that organic aerosols are probably insufficient to explain all of the observed CH_3CHO levels in the remote FT. We speculate the existence of unmeasured gas-phase organic compounds that are responsible for the observed CH_3CHO. The total removal rate of CH_3CHO ranges from ~42 ppt/hr in the MBL to ~6 ppt/hr in the upper FT (both instantaneous rates), implying a possibly widespread missing reactive carbon source in the remote troposphere on the order of 0.1–0.7 ppb C/day (24-hr average). The challenge for future research is to discover the origin and identity of these precursors.

References

Anderson, D. C., Nicely, J. M., Wolfe, G. M., Hanisco, T. F., Salawitch, R. J., Canty, T. P., et al. (2017). Formaldehyde in the tropical western Pacific: Chemical sources and sinks, convective transport, and representation in CAM-Chem and the CCMI models. *Journal of Geophysical Research: Atmospheres*, *122*, 11,201–211,226. https://doi.org/10.1002/2016JD026121

Apel, E. C., Brauers, T., Koppmann, R., Bandowe, B., Boßmeyer, J., Holzke, C., et al. (2008). Intercomparison of oxygenated volatile organic compound measurements at the SAPHIR atmosphere simulation chamber. *Journal of Geophysical Research*, 113, D20307. https://doi.org/10.1029/2008JD009865

Apel, E. C., Hornbrook, R. S., Hills, A. J., Blake, N. J., Barth, M. C., Weinheimer, A., et al. (2015). Upper tropospheric ozone production from lightning NO_x-impacted convection: Smoke ingestion case study from the DC3 campaign. *Journal of Geophysical Research: Atmospheres*, *120*, 2505–2523. https://doi.org/10.1002/2014JD022121

Apel, E. C., Hills, A. J., Leub, R., Zindel, S., Eisele, S., & Riemer, D. D. (2003). A fast-GC/MS system to measure C_2 to C_4 carbonyls and methanol aboard aircraft. *Journal of Geophysical Research*, (D20), 108, 8794. https://doi.org/10.1029/2002JD003199

Arnold, S. R., Emmons, L. K., Monks, S. A., Law, K. S., Ridley, D. A., Turquety, S., et al. (2015). Biomass burning influence on high-latitude tropospheric ozone and reactive nitrogen in summer 2008: A multi-model analysis based on POLMIP simulations. *Atmospheric Chemistry and Physics*, *15*(11), 6047–6068. https://doi.org/10.5194/acp-15-6047-2015

Asher, W., & Wanninkhof, R. (1998). The effect of bubble-mediated gas transfer on purposeful dual-gaseous tracer experiments. *Journal of Geophysical Research*, *103*(C5), 10,555–10,560. https://doi.org/10.1029/98JC00245

Assaf, E., Sheps, L., Whalley, L., Heard, D., Tomas, A., Schoemaecker, C., & Fittschen, C. (2017). The reaction between CH_3O_2 and OH radicals: Product yields and atmospheric implications. *Environmental Science & Technology*, *51*(4), 2170–2177. https://doi.org/10.1021/acs.est.6b06265

Badia, A., Reeves, C. E., Baker, A. R., Saiz-Lopez, A., Volkamer, R., Koenig, T. K., et al. (2019). Importance of reactive halogens in the tropical marine atmosphere: a regional modelling study using WRF-Chem. *Atmospheric Chemistry and Physics*, *19*(5), 3161–3189. https://doi.org/10.5194/acp-19-3161-2019

Bates, M. S., Gonzalez-Flesca, N., Sokhi, R., & Cocheo, V. (2000). Atmospheric volatile organic compound monitoring. Ozone induced artefact formation. *Environmental Monitoring and Assessment*, *65*(1/2), 89–97. https://doi.org/10.1023/A:1006420412523

Beale, R., Dixon, J., Arnold, S., Liss, P., & Nightingale, P. (2013). Methanol, acetaldehyde, and acetone in the surface waters of the Atlantic Ocean. *Journal of Geophysical Research: Oceans*, *118*, 5412–5425. https://doi.org/10.1002/jgrc.20322

Beale, R., Dixon, J. L., Smyth, T. J., & Nightingale, P. D. (2015). Annual study of oxygenated volatile organic compounds in UK shelf waters. *Marine Chemistry*, *171*, 96–106. https://doi.org/10.1016/j.marchem.2015.02.013

Betterton, E. A., & Hoffmann, M. R. (1988). Henry's law constants of some environmentally important aldehydes. *Environmental Science & Technology*, *22*(12), 1415–1418. https://doi.org/10.1021/es00177a004

Blake, N. J., Blake, D. R., Simpson, I. J., Meinardi, S., Swanson, A. L., Lopez, J. P., et al. (2003). NMHCs and halocarbons in Asian continental outflow during the Transport and Chemical Evolution over the Pacific (TRACE-P) field campaign: Comparison with PEM-West B. *Journal of Geophysical Research*, *108*(D20), 8806. https://doi.org/10.1029/2002JD003367

Bossolasco, A., Faragó, E. P., Schoemaecker, C., & Fittschen, C. (2014). Rate constant of the reaction between CH_3O_2 and OH radicals. *Chemical Physics Letters*, *593*, 7–13. https://doi.org/10.1016/j.cplett.2013.12.052

Brock, C., Schröder, F., Kärcher, B., Petzold, A., Busen, R., & Fiebig, M. (2000). Ultrafine particle size distributions measured in aircraft exhaust plumes. *Journal of Geophysical Research*, *105*(D21), 26,555–26,567. https://doi.org/10.1029/2000JD900360

Burkholder, J. B., Sander, S. P., Abbatt, J., Barker, J. R., Huie, R. E., Kolb, C. E., et al. (2015). Chemical kinetics and photochemical data for use in atmospheric studies, Evaluation No. 18. JPL Publication 10-6, Jet Propulsion Laboratory, Pasadena, Http://Jpldataeval.Jpl.Nasa.Gov.

Carpenter, L. J., & Nightingale, P. D. (2015). Chemistry and release of gases from the surface ocean. *Chemical Reviews*, *115*(10), 4015–4034. https://doi.org/10.1021/cr5007123

Cazorla, M., Wolfe, G. M., Bailey, S. A., Swanson, A. K., Arkinson, H. L., & Hanisco, T. F. (2015). A new airborne laser-induced fluorescence instrument for in situ detection of formaldehyde throughout the troposphere and lower stratosphere. *Atmospheric Measurement Techniques*, *8*(2), 541–552. https://doi.org/10.5194/amt-8-541-2015

Chiu, R., Tinel, L., Gonzalez, L., Ciuraru, R., Bernard, F., George, C., & Volkamer, R. (2017). UV photochemistry of carboxylic acids at the air-sea boundary: A relevant source of glyoxal and other oxygenated VOC in the marine atmosphere. *Geophysical Research Letters*, *44*, 1079–1087. https://doi.org/10.1002/2016GL071240

Coburn, S., Ortega, I., Thalman, R., Blomquist, B., Fairall, C. W., & Volkamer, R. (2014). Measurements of diurnal variations and eddy covariance (EC) fluxes of glyoxal in the tropical marine boundary layer: Description of the Fast LED-CE-DOAS instrument. *Atmospheric Measurement Techniques*, *7*(10), 3579–3595. https://doi.org/10.5194/amt-7-3579-2014

Crosson, E. R. (2008). A cavity ring-down analyzer for measuring atmospheric levels of methane, carbon dioxide, and water vapor. *Applied Physics B*, *92*(3), 403–408. https://doi.org/10.1007/s00340-008-3135-y

Crounse, J. D., McKinney, K. A., Kwan, A. J., & Wennberg, P. O. (2006). Measurement of gas-phase hydroperoxides by chemical ionization mass spectrometry. *Analytical Chemistry*, *78*(19), 6726–6732. https://doi.org/10.1021/ac0604235

DeCarlo, P. F., Kimmel, J. R., Trimborn, A., Northway, M. J., Jayne, J. T., Aiken, A. C., et al. (2006). Field-deployable, high-resolution, time-of-flight aerosol mass spectrometer. *Analytical Chemistry*, *78*(24), 8281–8289. https://doi.org/10.1021/ac061249n

Diskin, G. S., Podolske, J. R., Sachse, G. W., & Slate, T. A. (2002). Open-path airborne tunable diode laser hygrometer. In *Proceedings of the SPIE*, (Vol. 4817, pp. 196–204). Bellingham, Washington: Soc. of Photoopt. Instrum. Eng.

Dixon, J., Beale, R., & Nightingale, P. (2013). Production of methanol, acetaldehyde, and acetone in the Atlantic Ocean. *Geophysical Research Letters*, 40, 4700–4705. https://doi.org/10.1002/grl.50922

Elkins, J. W., Fahey, D. W., Gilligan, J. M., Dutton, G. S., Baring, T. J., Volk, C. M., et al. (1996). Airborne gas chromatograph for in situ measurements of long-lived species in the upper troposphere and lower stratosphere. *Geophysical Research Letters*, 23(4), 347–350. https://doi.org/10.1029/96GL00244

Emmons, L. K., Arnold, S. R., Monks, S. A., Huijnen, V., Tilmes, S., Law, K. S., et al. (2015). The POLARCAT Model Intercomparison Project (POLMIP): Overview and evaluation with observations. *Atmospheric Chemistry and Physics*, 15(12), 6721–6744. https://doi.org/10.5194/acp-15-6721-2015

Faloona, I. C., Tan, D., Lesher, R. L., Hazen, N. L., Frame, C. L., Simpas, J. B., et al. (2004). A laser-induced fluorescence instrument for detecting tropospheric OH and HO_2: Characteristics and calibration. *Journal of Atmospheric Chemistry*, 47(2), 139–167. https://doi.org/10.1023/B:JOCH.0000021036.53185.0e

Fischer, E. V., Jacob, D. J., Yantosca, R. M., Sulprizio, M. P., Millet, D. B., Mao, J., et al. (2014). Atmospheric peroxyacetyl nitrate (PAN): A global budget and source attribution. *Atmospheric Chemistry and Physics*, 14(5), 2679–2698. https://doi.org/10.5194/acp-14-2679-2014

Goldan, P. D., Kuster, W. C., Williams, E., Murphy, P. C., Fehsenfeld, F. C., & Meagher, J. (2004). Nonmethane hydrocarbon and oxy hydrocarbon measurements during the 2002 New England Air Quality Study: NMHC AND OXY HC NEAQS 2002. *Journal of Geophysical Research*, 109, D21309. https://doi.org/10.1029/2003JD004455

Guenther, A. B., Jiang, X., Heald, C. L., Sakulyanontvittaya, T., Duhl, T., Emmons, L. K., & Wang, X. (2012). The Model of Emissions of Gases and Aerosols from Nature version 2.1 (MEGAN2.1): An extended and updated framework for modeling biogenic emissions. *Geoscientific Model Development*, 5(6), 1471–1492. https://doi.org/10.5194/gmd-5-1471-2012

Hodzic, A., Kasibhatla, P. S., Jo, D. S., Cappa, C. D., Jimenez, J. L., Madronich, S., & Park, R. J. (2016). Rethinking the global secondary organic aerosol (SOA) budget: Stronger production, faster removal, shorter lifetime. *Atmospheric Chemistry and Physics*, 16(12), 7917–7941. https://doi.org/10.5194/acp-16-7917-2016

Hoesly, R. M., Smith, S. J., Feng, L., Klimont, Z., Janssens-Maenhout, G., Pitkanen, T., et al. (2018). Historical (1750–2014) anthropogenic emissions of reactive gases and aerosols from the Community Emissions Data System (CEDS). *Geoscientific Model Development*, 11(1), 369–408. https://doi.org/10.5194/gmd-11-369-2018

Hornbrook, R. S., Hills, A. J., Riemer, D. D., Abdelhamid, A., Flocke, F. M., Hall, S. R., et al. (2016). Arctic springtime observations of volatile organic compounds during the OASIS-2009 campaign. *Journal of Geophysical Research: Atmospheres*, 121, 9789–9813. https://doi.org/10.1002/2015JD024360

Hu, W., Palm, B. B., Day, D. A., Campuzano-Jost, P., Krechmer, J. E., Peng, Z., et al. (2016). Volatility and lifetime against OH heterogeneous reaction of ambient isoprene-epoxydiols-derived secondary organic aerosol (IEPOX-SOA). *Atmospheric Chemistry and Physics*, 16(18), 11,563–11,580. https://doi.org/10.5194/acp-16-11563-2016

Jeffery, C. D., Robinson, I. S., & Woolf, D. K. (2010). Tuning a physically-based model of the air–sea gas transfer velocity. *Ocean Modelling*, 31(1-2), 28–35. https://doi.org/10.1016/j.ocemod.2009.09.001

Jenkin, M. E., Saunders, S. M., Wagner, V., & Pilling, M. J. (2003). Protocol for the development of the Master Chemical Mechanism, MCM v3 (Part B): Tropospheric degradation of aromatic volatile organic compounds. *Atmospheric Chemistry and Physics*, 3(1), 181–193. https://doi.org/10.5194/acp-3-181-2003

Johnson, M. T. (2010). A numerical scheme to calculate temperature and salinity dependent air-water transfer velocities for any gas. *Ocean Science*, 6(4), 913–932. https://doi.org/10.5194/os-6-913-2010

Kameyama, S., Tanimoto, H., Inomata, S., Tsunogai, U., Ooki, A., Takeda, S., et al. (2010). High-resolution measurement of multiple volatile organic compounds dissolved in seawater using equilibrator inlet–proton transfer reaction-mass spectrometry (EI–PTR-MS). *Marine Chemistry*, 122(1-4), 59–73. https://doi.org/10.1016/j.marchem.2010.08.003

Kay, J. E., Deser, C., Phillips, A., Mai, A., Hannay, C., Strand, G., et al. (2014). The Community Earth System Model (CESM) Large Ensemble Project: A community resource for studying climate change in the presence of internal climate variability. *Bulletin of the American Meteorological Society*, 96(8), 1333–1349. https://doi.org/10.1175/BAMS-D-13-00255.1

Kieber, R., Zhou, X., & Mopper, K. (1990). Formation of carbonyl compounds from UV-induced photodegradation of humic substances in natural waters: Fate of riverine carbon in the sea. *Limnology and Oceanography*, 35(7), 1503–1515. https://doi.org/10.4319/lo.1990.35.7.1503

Kieber, R., Zhou, X., & Mopper, K. (2003). Formation of carbonyl compounds from UV-induced photodegradation of humic substances in natural waters: Fate of riverine carbon in the sea. *Limnology and Oceanography*, 35(7), 1503–1515. https://doi.org/10.4319/lo.1990.35.7.1503

Koenig, T. K., Volkamer, R., Baidar, S., Dix, B., Wang, S., Anderson, D. C., et al. (2017). BrO and inferred Bry profiles over the western Pacific: Relevance of inorganic bromine sources and a Bry minimum in the aged tropical tropopause layer. *Atmospheric Chemistry and Physics*, 17(24), 15,245–15,270. https://doi.org/10.5194/acp-17-15245-2017

Kupc, A., Williamson, C., Wagner, N. L., Richardson, M., & Brock, C. A. (2018). Modification, calibration, and performance of the Ultra-High Sensitivity Aerosol Spectrometer for particle size distribution and volatility measurements during the Atmospheric Tomography Mission (ATom) airborne campaign. *Atmospheric Measurement Techniques*, 11(1), 369–383. https://doi.org/10.5194/amt-11-369-2018

Lamarque, J. F., Emmons, L. K., Hess, P. G., Kinnison, D. E., Tilmes, S., Vitt, F., et al. (2012). CAM-chem: Description and evaluation of interactive atmospheric chemistry in the Community Earth System Model. *Geoscientific Model Development*, 5(2), 369–411. https://doi.org/10.5194/gmd-5-369-2012

Lee, T., Lagerloef, G., Gierach, M. M., Kao, H.-Y., Yueh, S., & Dohan, K. (2012). Aquarius reveals salinity structure of tropical instability waves: Aquarius reveals salinity of TIWs. *Geophysical Research Letters*, 39, L12610. https://doi.org/10.1029/2012GL052232

Liss, P. S., & Slater, P. G. (1974). Flux of gases across the air-sea interface. *Nature*, 247(5438), 181–184. https://doi.org/10.1038/247181a0

Mackay, D., & Yeun, A. T. K. (1983). Mass transfer coefficient correlations for volatilization of organic solutes from water. *Environmental Science & Technology*, 17(4), 211–217. https://doi.org/10.1021/es00110a006

Maritorena, S., Siegel, D. A., & Peterson, A. R. (2002). Optimization of a semianalytical ocean color model for global-scale applications. *Applied Optics*, 41(15), 2705–2714. https://doi.org/10.1364/AO.41.002705

McManus, J. B., Nelson, D. D., Shorter, J. H., Jimenez, R., Herndon, S., Saleska, S., & Zahniser, M. (2005). A high precision pulsed quantum cascade laser spectrometer for measurements of stable isotopes of carbon dioxide. *Journal of Modern Optics*, 52(16), 2309–2321. https://doi.org/10.1080/09500340500303710

Millet, D. B., Guenther, A., Siegel, D. A., Nelson, N. B., Singh, H. B., de Gouw, J. A., et al. (2010). Global atmospheric budget of acetaldehyde: 3-D model analysis and constraints from in-situ and satellite observations. *Atmospheric Chemistry and Physics*, *10*(7), 3405–3425. https://doi.org/10.5194/acp-10-3405-2010

Molina, M. J., Ivanov, A. V., Trakhtenberg, S., & Molina, L. T. (2004). Atmospheric evolution of organic aerosol. *Geophysical Research Letters*, *31*, L22104. https://doi.org/10.1029/2004GL020910

Mopper, K., & Stahovec, W. L. (1986). Sources and sinks of low molecular weight organic carbonyl compounds in seawater. *Marine Chemistry*, *19*(4), 305–321. https://doi.org/10.1016/0304-4203(86)90052-6

Mopper, K., Zhou, X., Kieber, R. J., Kieber, D. J., Sikorski, R. J., & Jones, R. D. (1991). Photochemical degradation of dissolved organic carbon and its impact on the oceanic carbon cycle. *Nature*, *353*(6339), 60–62. https://doi.org/10.1038/353060a0

Moxim, W. J., Levy, H., & Kasibhatla, P. S. (1996). Simulated global tropospheric PAN: Its transport and impact on NO$_x$. *Journal of Geophysical Research*, *101*(D7), 12,621–12,638. https://doi.org/10.1029/96JD00338

Nault, B. A., Campuzano-Jost, P., Day, D. A., Schroder, J. C., Anderson, B., Beyersdorf, A. J., et al. (2018). Secondary organic aerosol production from local emissions dominates the organic aerosol budget over Seoul, South Korea, during KORUS-AQ. *Atmospheric Chemistry and Physics Discussions*, *18*, 17,769–17,800. https://doi.org/10.5194/acp-2018-838

Nightingale, P. D., Malin, G., Law, C. S., Watson, A. J., Liss, P. S., Liddicoat, M. I., et al. (2000). In situ evaluation of air-sea gas exchange parameterizations using novel conservative and volatile tracers. *Global Biogeochemical Cycles*, *14*(1), 373–387. https://doi.org/10.1029/1999GB900091

Northway, M. J., de Gouw, J. A., Fahey, D. W., Gao, R. S., Warneke, C., Roberts, J. M., & Flocke, F. (2004). Evaluation of the role of heterogeneous oxidation of alkenes in the detection of atmospheric acetaldehyde. *Atmospheric Environment*, *38*(35), 6017–6028. https://doi.org/10.1016/j.atmosenv.2004.06.039

Ogawa, H., & Tanoue, E. (2003). Dissolved organic matter in oceanic waters. *Journal of Oceanography*, *59*(2), 129–147. https://doi.org/10.1023/A:1025528919771

Read, K. A., Carpenter, L. J., Arnold, S. R., Beale, R., Nightingale, P. D., Hopkins, J. R., et al. (2012). Multiannual observations of acetone, methanol, and acetaldehyde in remote tropical Atlantic air: Implications for atmospheric OVOC budgets and oxidative capacity. *Environmental Science & Technology*, *46*(20), 11,028–11,039. https://doi.org/10.1021/es302082p

Rudich, Y. (2003). Laboratory perspectives on the chemical transformations of organic matter in atmospheric particles. *Chemical Reviews*, *103*(12), 5097–5124. https://doi.org/10.1021/cr020508f

Ryerson, T., Williams, E., & Fehsenfeld, F. (2000). An efficient photolysis system for fast-response NO$_2$ measurements. *Journal of Geophysical Research*, *105*(D21), 26,447–26,461. https://doi.org/10.1029/2000JD900389

Schlundt, C., Tegtmeier, S., Lennartz, S. T., Bracher, A., Cheah, W., Krüger, K., et al. (2017). Oxygenated volatile organic carbon in the western Pacific convective center: Ocean cycling, air–sea gas exchange and atmospheric transport. *Atmospheric Chemistry and Physics*, *17*(17), 10837–10854. https://doi.org/10.5194/acp-17-10837-2017

Schroder, J. C., Campuzano-Jost, P., Day, D. A., Shah, V., Larson, K., Sommers, J. M., et al. (2018). Sources and secondary production of organic aerosols in the northeastern United States during winter. *Journal of Geophysical Research: Atmospheres*, *123*, 7771–7796. https://doi.org/10.1029/2018JD028475

Seinfeld, J. H., & Pandis, S. N. (2012). *Atmospheric Chemistry and Physics: From Air Pollution to Climate Change*. New York: John Wiley.

Shetter, R. E., & Müller, M. (1999). Photolysis frequency measurements using actinic flux spectroradiometry during the PEM-Tropics mission: Instrumentation description and some results. *Journal of Geophysical Research*, *104*(D5), 5647–5661. https://doi.org/10.1029/98JD01381

Singh, H. B., Chen, Y., Staudt, A., Jacob, D., Blake, D., Heikes, B., & Snow, J. (2001). Evidence from the Pacific troposphere for large global sources of oxygenated organic compounds. *Nature*, *410*(6832), 1078–1081. https://doi.org/10.1038/35074067

Singh, H. B., Condon, E., Vedder, J., O'Hara, D., Ridley, B. A., Gandrud, B. W., et al. (1990). Peroxyacetyl nitrate measurements during CITE 2: Atmospheric distribution and precursor relationships. *Journal of Geophysical Research*, *95*(D7), 10,163–10,178. https://doi.org/10.1029/JD095iD07p10163

Singh, H. B., Tabazadeh, A., Evans, M. J., Field, B. D., Jacob, D. J., Sachse, G., et al. (2003). Oxygenated volatile organic chemicals in the oceans: Inferences and implications based on atmospheric observations and air-sea exchange models. *Geophysical Research Letters*, *30*(16), 1862. https://doi.org/10.1029/2003GL017933

Sinha, V., Williams, J., Meyerhöfer, M., Riebesell, U., Paulino, A. I., & Larsen, A. (2007). Air-sea fluxes of methanol, acetone, acetaldehyde, isoprene and DMS from a Norwegian fjord following a phytoplankton bloom in a mesocosm experiment. *Atmospheric Chemistry and Physics*, *7*(3), 739–755. https://doi.org/10.5194/acp-7-739-2007

Soloviev, A., & Schluessel, P. (2002). A model of air-sea gas exchange incorporating the physics of the turbulent boundary layer and the properties of the sea surface. In *Gas Transfer at Water Surfaces*, *Geophysical Monograph Series* (Vol. 127, pp. 141–146). Washington, DC: American Geophysical Union.

Staudt, A. C., Jacob, D. J., Ravetta, F., Logan, J. A., Bachiochi, D., Krishnamurti, T. N., et al. (2003). Sources and chemistry of nitrogen oxides over the tropical Pacific. *Journal of Geophysical Research*, *108*(D2), 8239. https://doi.org/10.1029/2002JD002139

Swan, C. M., Siegel, D. A., Nelson, N. B., Carlson, C. A., & Nasir, E. (2009). Biogeochemical and hydrographic controls on chromophoric dissolved organic matter distribution in the Pacific Ocean. *Deep Sea Research Part I: Oceanographic Research Papers*, *56*(12), 2175–2192. https://doi.org/10.1016/j.dsr.2009.09.002

Thornberry, T., & Abbatt, J. P. D. (2004). Heterogeneous reaction of ozone with liquid unsaturated fatty acids: Detailed kinetics and gas-phase product studies. *Physical Chemistry Chemical Physics*, *6*(1), 84–93. https://doi.org/10.1039/B310149E

Tilmes, S., Lamarque, J. F., Emmons, L. K., Kinnison, D. E., Ma, P. L., Liu, X., et al. (2015). Description and evaluation of tropospheric chemistry and aerosols in the Community Earth System Model (CESM1.2). *Geoscientific Model Development*, *8*(5), 1395–1426. https://doi.org/10.5194/gmd-8-1395-2015

Volkamer, R., Baidar, S., Campos, T., Coburn, S., DiGangi, J. P., Dix, B., et al. (2015). Aircraft measurements of BrO, IO, glyoxal, NO$_2$, H$_2$O, O$_2$–O$_2$ and aerosol extinction profiles in the tropics: Comparison with aircraft-/ship-based in situ and lidar measurements. *Atmospheric Measurement Techniques*, *8*(5), 2121–2148. https://doi.org/10.5194/amt-8-2121-2015

Wang, S., Schmidt, J. A., Baidar, S., Coburn, S., Dix, B., Koenig, T. K., et al. (2015). Active and widespread halogen chemistry in the tropical and subtropical free troposphere. *Proceedings of the National Academy of Sciences of the United States of America*, *112*(30), 9281–9286. https://doi.org/10.1073/pnas.1505142112

Wiedinmyer, C., Akagi, S. K., Yokelson, R. J., Emmons, L. K., Al-Saadi, J. A., Orlando, J. J., & Soja, A. J. (2011). The Fire INventory from NCAR (FINN): A high resolution global model to estimate the emissions from open burning. *Geoscientific Model Development*, *4*(3), 625–641. https://doi.org/10.5194/gmd-4-625-2011

Williamson, C., Kupc, A., Wilson, J., Gesler, D. W., Reeves, J. M., Erdesz, F., et al. (2018). Fast time response measurements of particle size distributions in the 3–60 nm size range with the nucleation mode aerosol size spectrometer. *Atmospheric Measurement Techniques*, *11*(6), 3491–3509. https://doi.org/10.5194/amt-11-3491-2018

Wofsy, S. C., Afshar, S., Allen, H. M., Apel, E., Asher, E. C., Barletta, B., et al. (2018). *ATom: Merged Atmospheric Chemistry, Trace Gases, and Aerosols*. Oak Ridge, Tennessee: ORNL DAAC. https://doi.org/10.3334/ornldaac/1581

Yang, M., Beale, R., Liss, P., Johnson, M., Blomquist, B., & Nightingale, P. (2014). Air–sea fluxes of oxygenated volatile organic compounds across the Atlantic Ocean. *Atmospheric Chemistry and Physics*, *14*(14), 7499–7517. https://doi.org/10.5194/acp-14-7499-2014

Zhou, X., & Mopper, K. (1997). Photochemical production of low-molecular-weight carbonyl compounds in seawater and surface micro-layer and their air-sea exchange. *Marine Chemistry*, *56*(3-4), 201–213. https://doi.org/10.1016/S0304-4203(96)00076-X